

## Electrical resistivity and structure of amorphous Ge<sub>100-x</sub> Sb<sub>x</sub> thin films

M S Abo Ghazala, Y L El-Kady, M M El-Zaidia, M M El-Ocker<sup>(1)</sup>  
and E M Farag

Physics Department, Faculty of Science, Menoufia University, Egypt

Received 7 October 1994, accepted 9 June 1995

**Abstract** : Thin films of amorphous Ge<sub>100-x</sub> Sb<sub>x</sub>, where  $x = 5, 10, 50, 80, 90$  and  $95$  at. %, were prepared by the flash evaporation technique. The temperature dependence of the resistivity of these films reveals two activation energies for conduction in the temperature range  $300-580$  K. The temperature of the amorphous-crystalline transition ( $T_{\text{kin}}$ ), shifts to higher value as the Sb-content increases. The disorder-order transition occurred when the films were annealed at  $100, 130, 140$  and  $150^\circ\text{C}$  for different times. The X-ray results revealed crystalline Ge, Sb and Ge Sb. phases. It was found that the values of the resistivity and the activation energy decrease as a result of raising the annealing temperature and/or Sb content.

**Keywords** : Electrical resistivity, structure, amorphous thin films

**PACS Nos.** : 73.61.Jc, 68.55.Jk,

### 1. Introduction

The most important parameters controlling the physical properties of amorphous germanium films and its alloys are the substrate temperature, the evaporation rate and the vacuum environment during the deposition [1]. To understand the electronic properties of amorphous semiconductors and insulators, a detailed knowledge of the structure of the investigated materials is required [2]. The diffraction experiments such as electrons X-rays or neutrons diffraction are usually used to study the structure. The density is an important parameter in the analysis of the diffraction data. A stable glassy state is appreciably less dense than the crystalline counterpart [3]. Amorphous semiconductors are suitable for studying the nature of randomness by comparison with crystals of the same material. Bulk-glassy samples are chemically ordered and comprise well-defined structural units. When the evaporated films are annealed at the glass-transition temperature, the density of the homopolar bonds decreases and the films approach the structure of the bulk glass [4]. It is reasonable to suppose that a change in the chemical bonding would affect the electronic properties of the material.

<sup>(1)</sup> Faculty of Science, El-Azhar University, Cairo, Egypt

The aim of this work is to study the temperature dependence of the electrical resistivity, the effect of antimony content on the electrical resistivity and the structure of thin films of amorphous  $\text{Ge}_{100-x}\text{Sb}_x$ .

## 2. Experimental

Bulk samples of the system  $\text{Ge}_{100-x}\text{Sb}_x$ , where  $x = 5, 10, 50, 80, 90$  and  $95$  at. %, were prepared by the melt quenching technique. Appropriate proportions of 99.999% purity elements were mixed together in silica ampoules which were sealed under vacuum at  $10^{-4}$  torr. Each ampoule was heated at  $1100^\circ\text{C}$  for 10 hour and rocked from time to time to ensure a good mixing of the constituents, and subsequently quenched rapidly in ice-water. Amorphous thin films of thickness of order  $2000 \text{ \AA}$  were prepared by the flash evaporation technique at room temperature from the ingot material. Using X-ray diffraction, the evaporated films were found to be in amorphous state. The electrical resistivity as a function of temperature was recorded using the two probe method. The contact between the terminals of the resistance measurements and the films was silver paste. Accordingly, the contact effects and space charge are minimized.

## 3. Results and discussion

Figure 1 shows the temperature dependence of the resistivity of amorphous  $\text{Ge}_{100-x}\text{Sb}_x$  thin films, where  $x = 5, 10, 50, 80, 90$  and  $95$  at. %. This dependence shows an abrupt and sharp

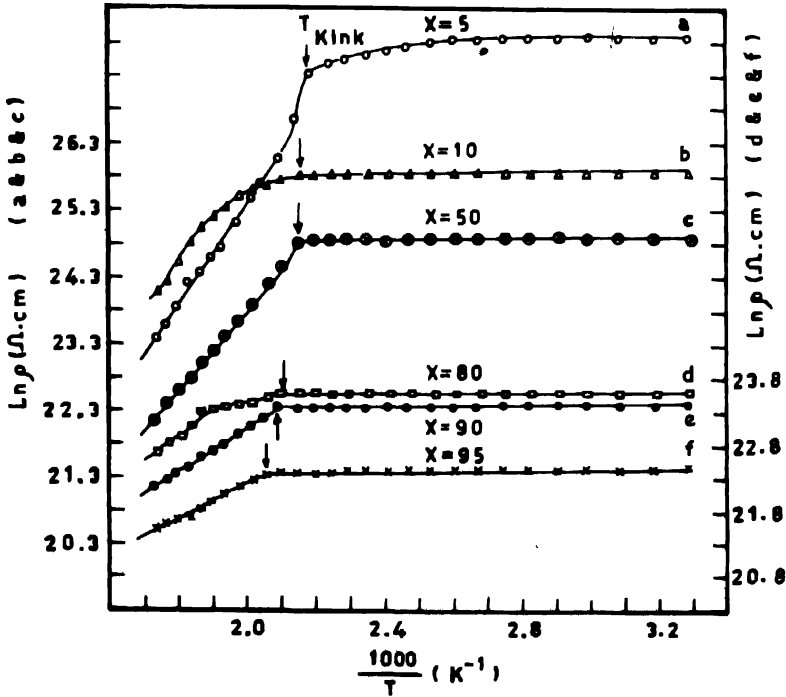


Figure 1. Arrhenius plot of temperature dependence of the resistivity for films of  $\text{Ge}_{100-x}\text{Sb}_x$  system ( $x = 5, 10, 50, 80, 90$  and  $95$  at. %).

decreasing of the resistivity at a certain temperature  $T_{kink}$  which is higher than the glass transition temperature  $T_g$ . Two straight lines were obtained confirming the semiconducting behaviour and obeying the Arrhenius type equation,

$$\sigma = \sigma_0 \exp (-E/KT),$$

where  $\sigma$  is the conductivity at any temperature,  $\sigma_0$  is a constant and  $E$  is the activation energy for conduction. This means that every composition transforms from amorphous to

Table 1. The activation energies and the temperature of transitions for a-Ge<sub>100-x</sub>Sb<sub>x</sub> thin films.

X	$E_a$ (ev)	$E_c$ (ev)	$T_{kink}$ (k)
5	0.097	0.616	454
10	0.071	0.595	463
50	0.058	0.420	465
80	Th	0.305	474
90	Th	0.263	476
95	Th.	0.232	485

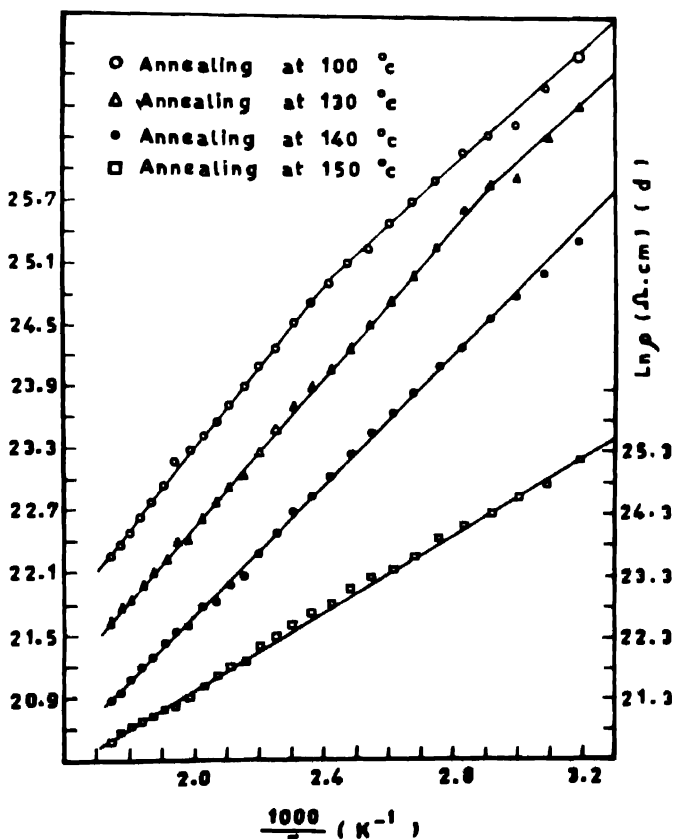


Figure 2a. Arrhenius plot of temperature dependence of the resistivity after annealing at 100, 130, 140 and 150°C, for films of Ge<sub>100-x</sub>Sb<sub>x</sub> system, x = 5%.

crystalline state  $a$ - $c$  transition. The obtained activation energy for each phase are related to the conduction mechanism of the corresponding phase. The values of the activation energy

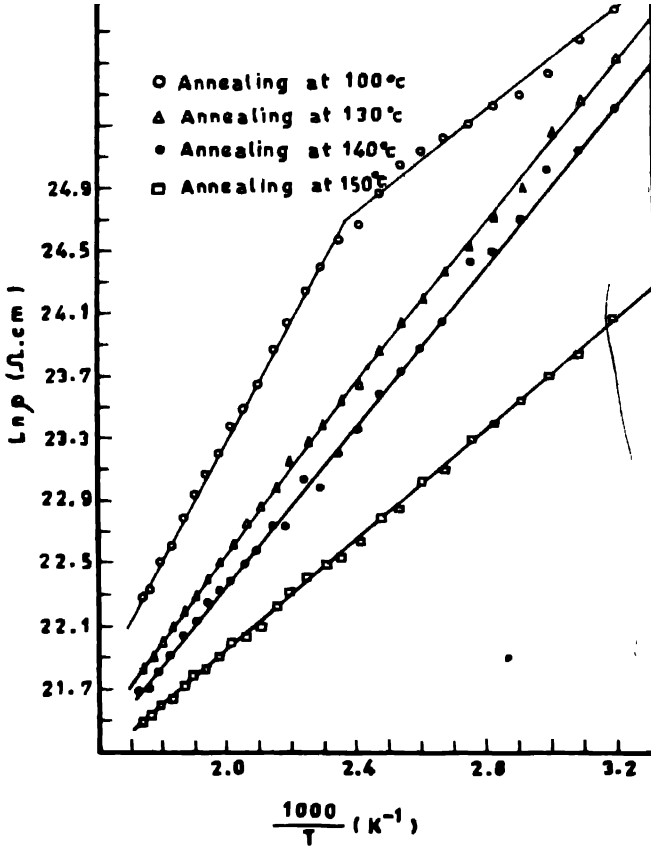


Figure 2b. Arrhenius plot of temperature dependence of the resistivity after annealing at 100, 130, 140 and 150°C, for films of  $\text{Ge}_{100-x}\text{Sb}_x$  system,  $x = 10\%$ .

of amorphous phase  $E_a$ , the activation energy of crystalline phase  $E_c$  and the temperature at which  $a$ - $c$  transition occurs  $T_{kink}$  for all compositions are given in Table 1. It is shown that  $E_a$  slightly decreases as the Sb content increases from 5 to 50 at. %. This decrease may be due to increase of the band tailing of the localized states which leads to a reduction in the actual gap. With increasing the Sb content from 80 up to 95 at. %, the activation energy  $E_a$  becomes very small and comes close to the order of thermal activation energy. This may be due to the Fermi energy passes through the conduction band edge or very close to it [5]. It is obvious also that the activation energy of crystalline phase  $E_c$  decreases with increasing the Sb content. This is due to the increase of the localized state density within the band gap. The shift of  $T_{kink}$  to higher values with increasing the Sb content means that the time required for  $a$ - $c$  transformation will increase at constant heating rate. In other words, the heat consumed during this transformation must be increased as the Sb content increases.

Figure (2a,b) shows the temperature dependence of the electrical resistivity for  $x = 5$  and 10 at. % samples annealed at 100, 130, 140 and 150°C for 5 hours. The annealing

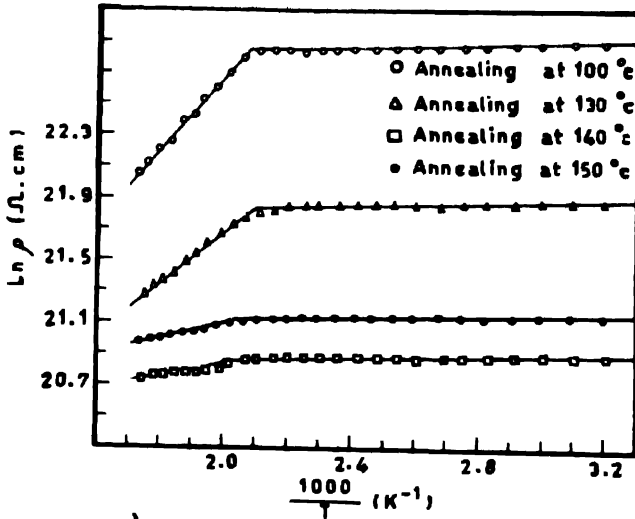


Figure 3a. Arrhenius plot of temperature dependence of the resistivity after annealing at 100, 130, 140 and 150°C, for films of  $\text{Ge}_{100-x}\text{Sb}_x$  system,  $x = 50\%$

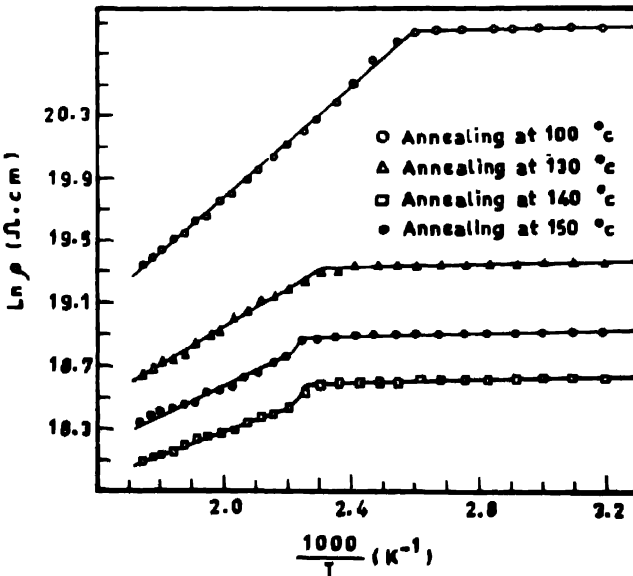


Figure 3b. Arrhenius plot of temperature dependence of the resistivity after annealing at 100, 130, 140 and 150°C, for films of  $\text{Ge}_{100-x}\text{Sb}_x$  system,  $x = 80\%$ .

temperatures were selected between the glass transition temperature  $T_g$  and the crystallization temperatures  $T_c$  as detected from DTA thermograms. It is seen from Figure 2

that the temperature dependence of the electrical resistivity still follows an Arrhenius equation. For films ( $x = 5$  and  $10$  at. %) annealed at  $100^\circ\text{C}$ , two activation energies ( $E_a$  and

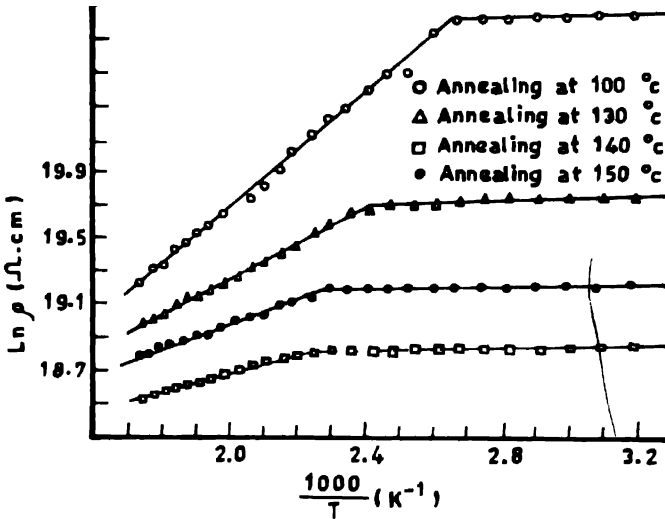


Figure 3c. Arrhenius plot of temperature dependence of the resistivity after annealing at  $100, 130, 140$  and  $150^\circ\text{C}$ , for films of  $\text{Ge}_{100-x}\text{Sb}_x$  system,  $x = 90\%$ .

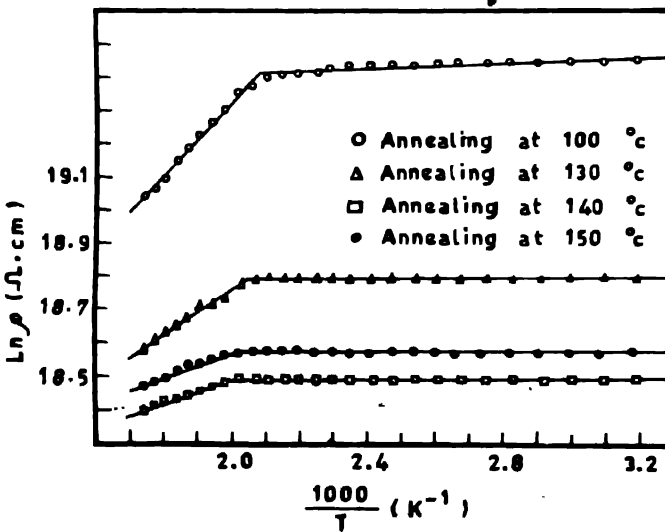


Figure 3d. Arrhenius plot of temperature dependence of the resistivity after annealing at  $100, 130, 140$  and  $150^\circ\text{C}$ , for films of  $\text{Ge}_{100-x}\text{Sb}_x$  system,  $x = 95\%$ .

$E_c$ ) were obtained while the films annealed at  $130, 140$  and  $150^\circ\text{C}$  show only one activation energy ( $E_c$ ). This is due to the fast  $a$ - $c$  transformation at higher temperatures. For Films of higher Sb content ( $x = 50, 80, 90$  and  $95$  at. %), two activation energies of amorphous and

crystalline phases  $E_a$  and  $E_c$  were obtained all over the range of annealing temperature as shown in Figure (3a,b,c,d). Also the transition temperature  $T_{kink}$  is shifted to higher value and the DC electrical resistivity decreases as the annealing temperature increases. To show the effect of annealing on the structure of the films, a- $Ge_{10}Sb_{90}$  thin film annealed at 150 and 320°C for different times was investigated by X-ray as shown in Figure 4. The detected

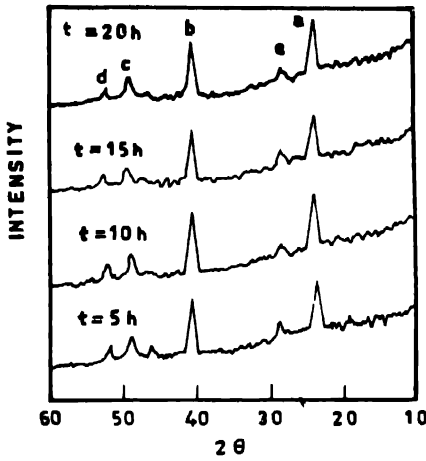


Figure 4a. X-ray diffraction records for amorphous  $Ge_{10}Sb_{90}$  thin film annealed for different times at 150°C

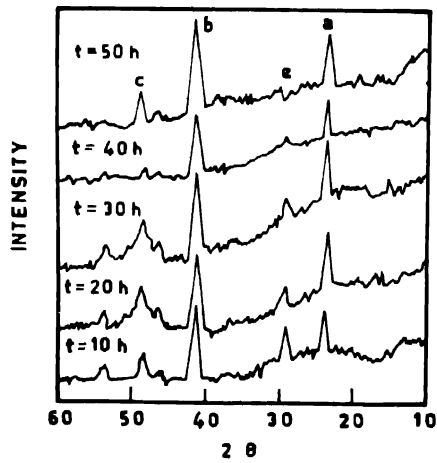


Figure 4b. X-ray diffraction records for amorphous  $Ge_{10}Sb_{90}$  thin film annealed for different times at 320°C.

peaks reveal that some partial crystallization occurs after annealing. The growth of these peaks with increasing the annealing time shows the growth of the crystalline phase on the expense of the amorphous one. The detected crystalline phases were found to be Ge in the tetragonal form and Sb in the hexagonal form. Also, a new crystalline phase in the hexagonal form was appeared and it may be due to Ge Sb phase as shown in Table 2.

Table 2. X-ray crystallographic of sample  $Ge_{10}Sb_{90}$  after annealing for different times (h) at 150°C.

Time of annealing <i>t</i> (h)	Experimental			ASTM cards			
	Crystal phase	$2\theta$	<i>gA</i>	Crystal phase	<i>gA</i>	( <i>hkl</i> )	Crystal
(a)	Unknown	23.8	3.73	—	—	—	—
(b)	Sb	40.2	2.24	Sb	2.248	(014)	Hexagonal
5 (c)	Ge	48.8	1.864	Ge	1.856	(301)	Tetragon.
(d)	Ge	51.8	1.762	Ge	1.745	(004)	Tetragon.
(e)	Ge	28.8	3.096	Ge	3.01	(012)	Tetragon.

(Table 2. Cont'd.)

Time of annealing $t$ (h)	Experimental			ASTM cards			Crystal
	Crystal phase	$2\theta$	$gA$	Crystal phase	$gA$	( $hkl$ )	
(a)	Unknown	23.7	3.749	—	—	—	—
(b)	Sb	40.2	2.24	Sb	2.248	(014)	Hexagonal
10 (c)	Ge	48.7	1.867	Ge	1.87	(310)	Tetragon
(d)	Ge	51.8	1.762	Ge	1.745	(004)	Tetragon.
(e)	Ge	28.8	3.096	Sb	3.109	(102)	Hexagon.
(a)	Unknown	23.8	3.734	—	—	—	—
(b)	Sb	40.2	2.24	Sb	2.248	(014)	Hexagonal
15 (c)	—	48.5	1.867	{ Ge Sb }	{ 1.87 1.878 }	{ (310) (006) }	{ Tetr. Hex. }
(d)	Ge	52	1.754	Ge	1.745	(004)	Tetragon.
(e)	Ge	28.6	3.014	Ge	3.01	(012)	Tetragon
(a)	Unknown	23.7	3.749	—	—	—	—
(b)	Sb	40.2	2.245	Sb	2.248	(014)	Hexagonal
20 (c)	—	48.5	1.867	{ Ge Sb }	{ 1.87 1.878 }	{ (310) (006) }	{ Tetr Hex }
(d)	Ge	51.7	1.766	Ge	1.745	(004)	Tetragon.
(e)	Sb	28.9	3.085	Sb	3.109	(102)	Hexagonal

## References

- [1] Peter Viscor *J. Non-Cryst. Solids* **101** 156 (1988)
- [2] V Heine, D W Bullet, R Haydock and M J Kelly *Solid. State Phys.* **35** 1 (1980)
- [3] T M Donovan, F J Ashley and W F Spicer *Phys. Lett.* **A32** 85 (1970)
- [4] R A Street, R J Nemanich and G A N Connell *Phys. Rev.* **12** 6915 (1978)
- [5] N F Mott and E A Davis *Electronic Processes in Non-Crystalline Materials* 2nd edn (Oxford Clarendon) p 20 (1979)